© 2018. Published by The Company of Biologists Ltd | Journal of Experimental Biology (2018) 221, jeb179416. doi:10.1242/jeb.179416

RESEARCH ARTICLE

Vocal tract modelling in fallow deer: are male groans nasalized?

D. Reby[1,*], M. T. Wyman[1,2], R. Frey[3], B. D. Charlton[4], J. P. Dalmont[5] and J. Gilbert[5]

ABSTRACT

Males of several species of deer have a descended and mobile larynx, resulting in an unusually long vocal tract, which can be further extended by lowering the larynx during call production. Formant frequencies are lowered as the vocal tract is extended, as predicted when approximating the vocal tract as a uniform quarter wavelength resonator. However, formant frequencies in polygynous deer follow uneven distribution patterns, indicating that the vocal tract configuration may in fact be rather complex. We CT-scanned the head and neck region of two adult male fallow deer specimens with artificially extended vocal tracts and measured the cross-sectional areas of the supra-laryngeal vocal tract along the oral and nasal tracts. The CT data were then used to predict the resonances produced by three possible configurations, including the oral vocal tract only, the nasal vocal tract only, or combining the two. We found that the area functions from the combined oral and nasal vocal tracts produced resonances more closely matching the formant pattern and scaling observed in fallow deer groans than those predicted by the area functions of the oral vocal tract only or of the nasal vocal tract only. This indicates that the nasal and oral vocal tracts are both simultaneously involved in the production of a non-human mammal vocalization, and suggests that the potential for nasalization in putative oral loud calls should be carefully considered.

KEY WORDS: Acoustic variation, Mammal, Call production, Formant, Call nasalization, Mobile larynx, Vocal tract shape, Vocal tract resonance, Vocalization

INTRODUCTION

A key objective of mammalian vocal communication research is to determine whether the acoustic structure of vocal signals encodes functionally relevant information. To achieve this aim in a given species, it is important to understand how vocal signals are produced because any potential acoustic variation is primarily constrained by the biomechanical properties and dimensions of the caller's vocal anatomy (Fitch and Hauser, 2002). While the causal links between vocal production and acoustic variation are well established in human speech (Titze, 1989, 1994), the biomechanical and physiological sources of acoustic diversity in non-human animal signals remain poorly understood. Nonetheless, the generalization of the source-filter theory of human voice production (Fant, 1960) to non-human mammal vocal signals has significantly advanced our understanding of the acoustic structure of mammalian calls in light of their production mechanisms (reviewed by Taylor et al., 2016). According to this theory, voiced vocalizations are the result of a two-stage production process. First, the source signal is generated in the larynx by vocal fold vibration. The rate at which the glottis opens and closes determines the fundamental frequency (F0) of the vocalization (the main perceptual correlate of the pitch). The source signal is subsequently filtered by the supra-laryngeal vocal tract, whose resonance frequencies shape the spectral envelope of the radiated vocalization, creating broad bands of energy called 'formants' (Fitch, 2000a). Because F0 and formants are produced independently, they are subject to separate biomechanical constraints.

Recent anatomical investigations of mammalian supra-laryngeal vocal tracts have revealed an extensive diversity of vocal tract morphology, with, for example, elongated noses (Frey et al., 2007b), air sacs (Frey et al., 2007a) and descended larynges (Frey and Gebler, 2003), suggesting that vocal tract resonance is under strong selection pressure. Yet, to conclusively determine how such anatomical specializations affect vocal production requires 3D cineradiography to visualize call-synchronous internal dynamic changes in vocal tract shape and document the position of oscillating structures during call production (Fitch, 2000b). This approach is, however, logistically difficult – if not impossible – to perform on large wild animals. An alternative method is to obtain precise static vocal tract geometries from cadavers and use these data to simulate vocal tract dynamics and provide predictions of formant values for multiple vocal tract configurations. Several studies of non-human mammals have used this approach to predict the resonance characteristics of air spaces in the upper respiratory tract, showing good concordance with actual formant patterns in species-specific vocalizations (Adam et al., 2013; Carterette et al., 1979, 1984; Gamba et al., 2012; Gamba and Giacoma, 2006b; Koda et al., 2012; Riede et al., 2005). Studies investigating the evolutionary origins of speech have also used vocal tract models to predict the potential articulatory abilities of human ancestors (Boë et al., 2002; Lieberman et al., 1972) as well as non-human primates (Boë et al., 2002, 2017; Fitch et al., 2016). However, attempts at predicting vocal tract resonances from anatomical data remain scant and largely focused on primate species (Gamba et al., 2012; Gamba and Giacoma, 2006a; Koda et al., 2012; Riede et al., 2005), essentially because of the lack of data on vocal tract geometries available for non-human terrestrial mammals.

During the autumn breeding season, male fallow deer (*Dama dama*) produce high rates of sexually selected groan vocalizations (Briefer et al., 2010; McElligott and Hayden, 1999). Groans are characterized by a very low F0 and unevenly spaced and modulated formants that obey stereotyped distribution patterns, indicating that they are produced by a consistent but complex vocal tract shape (Reby et al., 1998; Vannoni and McElligott, 2007). Fallow bucks have a descended and mobile larynx that is retracted towards the sternum during groan production (Fitch and Reby, 2001; McElligott et al., 2006), thereby extending the vocal tract.

[1]School of Psychology, University of Sussex, Falmer, Brighton BN1 9QH, UK. [2]Department of Evolutionary Biology and Environmental Studies, University of Zurich, Winterthurerstrasse 190, 8057 Zurich, Switzerland. [3]Department of Reproduction Management, Leibniz Institute for Zoo and Wildlife Research (IZW), 10315 Berlin, Germany. [4]San Diego Zoo's Institute for Conservation Research, Escondido 92027, CA, USA. [5]Laboratoire d'Acoustique de l'Université du Mans, CNRS, 72085 le Mans, France.

*Author for correspondence (reby@sussex.ac.uk)

D.R., 0000-0001-9261-1711; M.T.W., 0000-0002-5684-4603; R.F., 0000-0002-6759-761X; B.D.C., 0000-0002-0218-7177

Received 16 February 2018; Accepted 21 June 2018

Journal of Experimental Biology (2018) 221, jeb179416. doi:10.1242/jeb.179416

The effect of vocal tract extension on formant frequency has been extensively documented in fallow deer (McElligott et al., 2006) and the closely related red deer (Fitch and Reby, 2001; Frey et al., 2012). As the animal extends its vocal tract, formants are lowered until they reach a minimal plateau corresponding to maximal extension, and formant frequency spacing is inversely correlated with the length of the vocal tract during extension (Fitch and Reby, 2001; McElligott et al., 2006).

Previous attempts at relating formant frequency spacing to vocal tract length have typically modelled the vocal tract as a simple tube of uniform diameter that is closed at the glottis and opened at the mouth (Charlton et al., 2011; Reby and McComb, 2003; Vannoni and McElligott, 2007; Fitch, 1997). Under these assumptions, the length of the vocal tract can be predicted from the formant frequency spacing (and vice versa) using the equation: $eVTL=c/2\times DF$, where eVTL is the estimated vocal tract length, c is the speed of sound in the vocal tract of 350 m s^{-1} and DF is the overall formant frequency spacing measured in the vocalization (Reby and McComb, 2003). Measurements of anatomical oral vocal tract length in adult male fallow deer (taken as the distance from the larynx to the tip of the snout) based on calibrated photographs have produced fully extended vocal tract lengths ranging between 46 and 54 cm (McElligott et al., 2006). Yet, the minimum formant spacing (DF) measured in male fallow deer groans varies between 326 and 281 Hz (Vannoni and McElligott, 2007), which, when the vocal tract is modelled as a simple cylindrical tube, corresponds to vocal tract lengths between 54 and 62 cm. This overestimation of the vocal tract length from the acoustic data indicates that the animal's vocal tract produces more/lower formants than expected from its anatomical length. Combined with the observation that formants are stereotypically unevenly spaced in groans (McElligott et al., 2006), this suggests the vocal tract configuration during groan production is more complex than previously assumed.

Here, we investigated the hypothesis that male fallow deer simultaneously use the oral and nasal vocal tracts as resonating systems during call production, allowing this species to produce a larger number of formants and a more complex formant pattern than predicted by a simple cylindrical tube model. To this end, we performed computed tomography (CT) scans of head-and-neck specimens of male fallow deer to achieve a more detailed description of the complex anatomical structure of the male fallow deer supra-laryngeal vocal tract. The specific aims of this investigation were threefold: (1) to describe the 3D geometry of the supra-laryngeal vocal tract in male fallow deer, including the oral and nasal vocal tracts, while the larynx is maximally retracted; (2) to predict the resonance patterns produced by the fully extended vocal tract configuration, simulating the effect of the involvement of the oral vocal tract only, of the nasal vocal tract only, or of the combined oral and nasal vocal tracts on formant patterns; and (3) to compare resonance patterns predicted by each of these configurations with formant patterns observed in actual vocalizations.

MATERIALS AND METHODS

A description of the anatomical terms used in this article is provided in the Glossary and a schematic representation of the mammalian vocal anatomy is provided in Fig. S1.

Specimen collection

Our measures of vocal tract area functions are based on CT scans from two adult male fallow deer, *Dama dama* (Linnaeus 1758). Male 1 was a 7-year-old buck that died from injuries sustained during a fight with rival males during the breeding season on 20 October 2011 in Home Park, London, UK. Male 2 was an 11-year-old buck culled by park staff during annual population control management practices on 7 February 2011 in Richmond Royal Park, London, UK. The two specimens had similar skeletal dimensions: lower mandible length (male 1: 21.0 cm, male 2: 20.3 cm) and lower hindleg length from the calcaneal tuber to the end of the metatarsus (male 1: 31 cm, male 2: 32.5 cm). Head-and-neck specimens of both individuals were obtained by separation between the 2nd and 3rd ribs. Specimens were chilled with ice within 2 h of death and were frozen at −20°C within 5 h of death.

Specimen preparation and CT scanning

Specimens were thawed, and water was flushed through the oral and nasal vocal tracts to remove debris and fluids and they were left upright to drain for about 30 min before scanning. Specimens were scanned with and without artificially extending the vocal tract. Vocal tract extension was achieved by maximally pulling the sternothyroid muscle and the trachea towards the sternum and fastening them to the sternum using a string. This recreated a naturalistic configuration of the fully extended vocal tract in male fallow deer.

Specimens were positioned as much as possible in configurations typical of vocalizing (see Fig. 1), although it was not possible to stretch the neck as much as desired (Fig. 2). The oral cavity was kept open using a block of Styrofoam. This affected the position of the tongue, which was pushed backward in an unnatural position in one

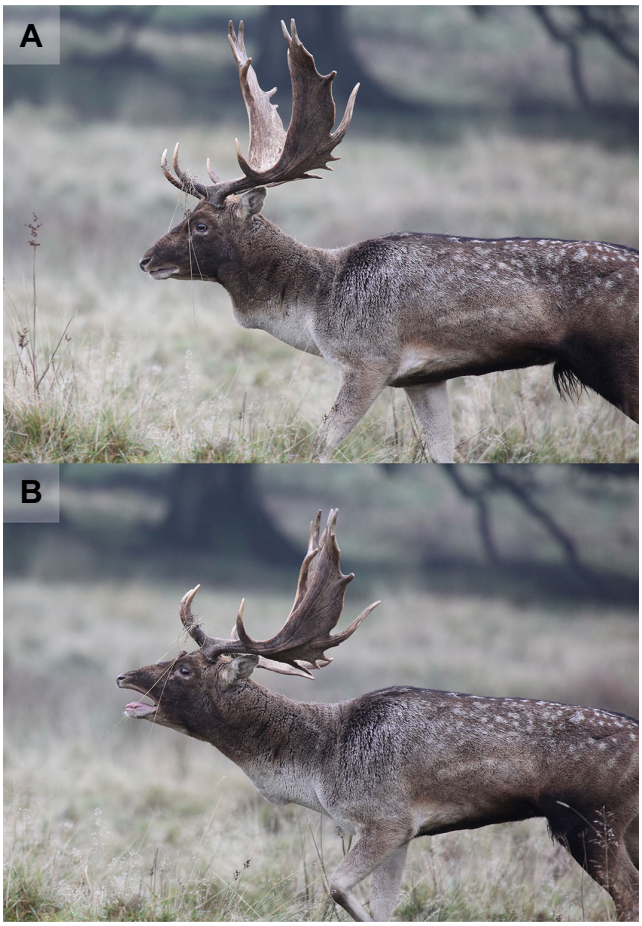

Fig. 1. Fallow deer buck in a pre-groaning posture and in a groaning posture during the annual rut. In the pre-groaning posture (A), the neck is not extended, the larynx is in its resting position and the mouth is closed. In the groaning posture (B), the neck is extended, the larynx is retracted and the mouth is open (no lip rounding). Photographs by Benjamin Pitcher.

Journal of Experimental Biology (2018) 221, jeb179416. doi:10.1242/jeb.179416

Glossary of anatomical terms used in this paper (based on Constantinescu and Schaller, 2012, and own descriptions)

Basihyoid
Unpaired, most ventral, transverse component of the hyoid apparatus intercalated between the paired suspension from the skull and the paired arms to the larynx.

Choanae
The 'internal nares', i.e. the two openings at the caudal end of the nasal cavity, where the paired nasal meatuses lead into the nasopharynx.

Cricoid cartilage
The most caudal, ring-shaped cartilage of the larynx that is attached to the trachea; it consists of a dorsal plate and a ventral arch.

Epiglottis
The most rostral cartilage of the larynx; during quiet breathing, it has a so-called intranarial position, i.e. it protrudes dorsally, through the intra-pharyngeal ostium, into the nasopharynx; during an open-mouth call, the larynx is withdrawn from the intra-pharyngeal ostium so that it is now positioned in the oropharynx.

Glottis
The vocal source of the larynx; it consists of the two vocal folds, ventral parts of the arytenoid cartilages and the vocal cleft in between the vocal folds; regarding the laryngeal cavity, it is positioned between the laryngeal vestibule rostrally and the infraglottic cavity caudally.

Hyoid apparatus
A framework of small rod-like bones connecting dorsally to the base of the skull, rostrally to the tongue and caudally to the larynx. It has three components: (1) the arms of the paired dorsal part flank the pharynx on both sides and suspend the entire hyoid apparatus from the skull base – it consists of several parts on both sides termed (dorsal to ventral): tympanohyoid, stylohyoid, epihyoid, ceratohyoid; (2) the arms of the paired caudal part connect to the larynx (in fallow deer via the two thyrohyoid ligaments) – it consists of one element per side termed the thyrohyoid; (3) the unpaired, transverse ventral part connects the two paired structures thereby forming a larger U-shaped fork for suspension from the skull dorsally and a smaller U-shaped fork for connection to the larynx caudally.

Intra-pharyngeal ostium
An opening in the soft palate, creating a passage between the nasopharynx and oropharynx; it is bordered by the palatopharyngeal muscle, which can constrict the intra-pharyngeal ostium.

Isthmus faucium
A narrow short passage between the mouth cavity and the oropharynx, bounded by the soft palate dorsally, the tongue ventrally and the palatoglossal arch (a symmetrical, dorsoventral mucosa fold between the soft palate and tongue) laterally.

Laryngeal entrance
The rostral entrance to the larynx, bounded by the epiglottis, the aryepiglottic folds and the corniculate processes of the arytenoid cartilages.

Nasopharynx
The nasal part of the pharynx, dorsal to the soft palate; it extends from the choanae to the intrapharyngeal ostium.

Oropharynx
The oral part of the pharynx, ventral to the soft palate; it extends from the isthmus faucium to the base of the epiglottis.

Pharynx
A musculomembraneous cross-way of the respiratory and digestive tracts between the oral and nasal cavities rostrally and the oesophagus and larynx caudally; for the sake of simplicity, and in contrast to textbooks, the pharynx is here not subdivided into three parts (nasal, oral and laryngeal) but only into two parts (nasal and oral).

Soft palate
Also known as the palatine velum, the soft palate is a soft tissue structure that is laterally fused to the pharyngeal walls; it completely separates the nasopharynx and oropharynx, except at the intra-pharyngeal ostium, which represents the only communication between the nasopharynx and oropharynx; like the pharynx, it extends from the choanae to the larynx.

Thyrohyoid
A paired caudal element of the hyoid apparatus that, together with the basihyoid, forms the smaller U-shaped fork for establishing the connection between the hyoid apparatus and the larynx.

Thyrohyoid ligament
Replaces the usual thyrohyoid articulation of most mammals by a ligamentous connection between the caudal tip of the thyrohyoid (of the hyoid apparatus) and the rostral horn of the thyroid cartilage on both sides.

Thyroid cartilage
The most superficial and largest cartilage of the larynx, unpaired. Its two lateral laminae are ventrally fused and enclose most of the laryngeal cavity in between them; its rostral horns connect the larynx to the thyrohyoid of the hyoid apparatus; its caudal horns articulate with the cricoid cartilage in the cricothyroid articulations.

Trachea
The windpipe, connecting the lungs to the larynx, extends from its bifurcation into the main bronchi caudally to the cricoid cartilage of the larynx rostrally.

of the specimens. The detrimental effect on the cross-sectional area measures was moderated by extrapolating the typical position of the tongue from other specimens and anatomical examinations.

Estimation of vocal tract area function

We measured the supra-laryngeal vocal tract area functions (the cross-sectional area at 1 cm steps along the length of the vocal tract; De Boer and Fitch, 2009) using the 3D curved Multi-Planar Representation viewer in Osirix (version 6.0, 64bits for Mac, www.osirix-viewer.com) and following the three-step method described in Kim et al. (2009). First, the oral and nasal vocal tract dorsoventral midlines were drawn manually using the '3D curved path' tool on a midsagittal section (Fig. 3A,D). Second, for each vocal tract, cross-sectional areas orthogonal to the midline were produced at 1 cm intervals from the glottis to the lips or nostrils (Fig. 3B–D). The vocal tract area was then measured in each cross-sectional slice using the closed polygon selection tool to delineate the VT area. Osirix automatically returned the area of the delineated zone (in cm^2). Each slice/measure was saved as an image file.

Prediction of vocal tract resonances

The position and amplitude of vocal tract resonances were predicted using the transfer matrix method (Chaigne and Kergomard, 2016),

Journal of Experimental Biology (2018) 221, jeb179416. doi:10.1242/jeb.179416

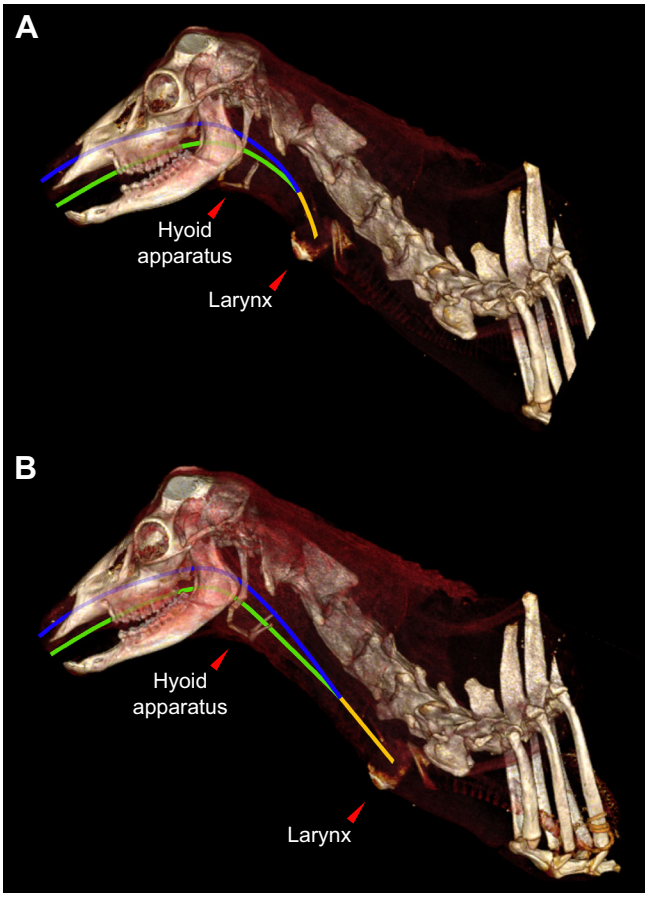

Fig. 2. Computed tomography (CT)-based 3D reconstructions of male 1. (A) Larynx and hyoid apparatus in the pre-groan (resting) position. (B) Larynx and hyoid apparatus in the groaning position at full artificial extension of the vocal tract. The larynx position is shifted caudally by approximately 12 cm. Yellow: common laryngopharyngeal tract; green: oropharynx and oral cavity; blue: nasopharynx and nasal cavities.

where the tube geometry is approximated as a series of cylindrical elements with variable cross-sections and 1 cm in length. The transfer matrix model is commonly used for modelling acoustic propagation in tube lattices. The method is appropriate when one dimension of the tube is substantially larger than the others, as in most mammalian vocal tracts: below a cut-off frequency F_{co} ($F_{co}\approx c/2D$, where c is the speed of sound and D is the largest transverse dimension), it can be assumed that only plane waves propagate. In this study, F_{co} is 4000 Hz as D remains below 4 cm in the fallow deer vocal tract. Assuming linear propagation, the internal acoustic field is perfectly defined by scalar quantities in the frequency domain: the complex amplitudes of the acoustic pressure P and of the acoustic volume velocity U. For a given cylindrical tube portion of length L and cross-sectional area A_o, a 2×2 matrix of complex elements relates vectors {**P**, **U**} on both sides (input, output) of the cylinder:

$$\begin{pmatrix} P_{in} \\ U_{in} \end{pmatrix} = \begin{pmatrix} \cos kL & i\,Z_c \sin kL \\ i\,Z_c^{-1} \sin kL & \cos kL \end{pmatrix} \begin{pmatrix} P_{out} \\ U_{out} \end{pmatrix}, \quad (1)$$

where $Z_c=\rho c/A_o$ is the characteristic impedance (where ρ and c are, respectively, the air density and the speed of sound at body temperature, and $k=\omega/c=2\pi F/c$ is the wave number).

For complex cylindrical geometry, the tube is broken down into smaller elementary cylindrical tubes. If the tube is described by N elementary cylindrical tubes, acoustic pressure and volume flow at the input and output of the tube are related by the matrix equal to the product of the N matrices of the elementary cells:

$$\begin{pmatrix} P_{in} \\ U_{in} \end{pmatrix} = \begin{pmatrix} A & B \\ C & D \end{pmatrix} \begin{pmatrix} P_{out} \\ U_{out} \end{pmatrix}. \quad (2)$$

It is thus possible to calculate the input impedance Z_{in}:

$$Z_{in} = \frac{P_{in}}{U_{in}} = \frac{A\,P_{out} + B\,U_{out}}{C\,P_{out} + D\,U_{out}} = \frac{A\,Z_{out} + B}{C\,Z_{out} + D}, \quad (3)$$

where $Z_{out}=P_{out}/U_{out}$ is the terminal impedance of the tube. If the tube is open (at the mouth and nostrils, for example), Z_{out} is the radiation impedance.

If several complex tubes are connected (for example, at the branching point of the oral and nasal tracts), there is continuity of the acoustic pressure and conservation of the acoustic volume flow. The particular frequencies where the input impedance magnitude reaches a local maximum correspond to the vocal tract resonances visible as formants in the spectral acoustic structure of the produced vocalization.

The input parameters are the area functions of the oral and nasal vocal tracts and the branching point of the tracts. The air temperature inside the fallow deer vocal tract, which affects the absolute frequency of predicted resonances (formant frequencies are proportional to the speed of sound in the air and thus to the square root of the absolute temperature) but not their relative frequency distribution, was set to 38°C. The model assumed wall damping of rigid walls and radiation impedance of an open-end, un-flanged tube (Chaigne and Kergomard, 2016).

Resonances were predicted for each male, based on the area functions of three possible configurations: (1) the oral vocal tract only (common laryngopharyngeal tract, oropharynx and oral cavity); (2) the nasal vocal tract only (common laryngopharyngeal tract, nasopharynx and nasal cavities); and (3) both the oral and nasal vocal tracts (common laryngopharyngeal tract, oropharynx, oral cavity, nasopharynx and nasal cavities).

The total cross-sectional areas of both (left and right) nasal cavities were approximated by doubling the cross-sectional areas measured for the left nasal cavity connecting to the left nostril. To approximate the potential effect of the partial opening of the sides of the mouth, we only included half of the portion of the oral cavity that is laterally open. The cross-sectional areas for this portion of the oral cavity were estimated by manually linking the upper lip to the lower lip.

RESULTS

Vocal tract anatomy

Anatomically, the complete vocal tract is composed of five distinct and connected sections, one of which is paired: (1) the common laryngopharyngeal tract, shared by the oral and nasal vocal tract, between the glottis and the intra-pharyngeal ostium; (2) the oropharynx, from the intra-pharyngeal ostium to the isthmus faucium (oropharyngeal tract); (3) the oral cavity, from the isthmus faucium to the mouth opening (oral tract); (4) the nasopharynx, from the intra-pharyngeal ostium to the choanae (nasopharyngeal tract); and (5) the paired nasal cavities, from the choanae to the nostrils (nasal tract). The oral vocal tract comprises parts 1, 2 and 3 and the nasal vocal tract parts 1, 4 and 5 (Fig. 2). The choanae and the isthmus faucium are located approximately at the same distance from the glottis.

In the resting configuration (Figs 1A, 2A and 4A,B), the pharynx, soft palate and thyrohyoid ligament are relaxed, and the larynx resides at the level of cervical vertebrae 2 and 3, but farther rostrally in male 2 than in male 1. Accordingly, the rostral end of the trachea

Journal of Experimental Biology (2018) 221, jeb179416. doi:10.1242/jeb.179416

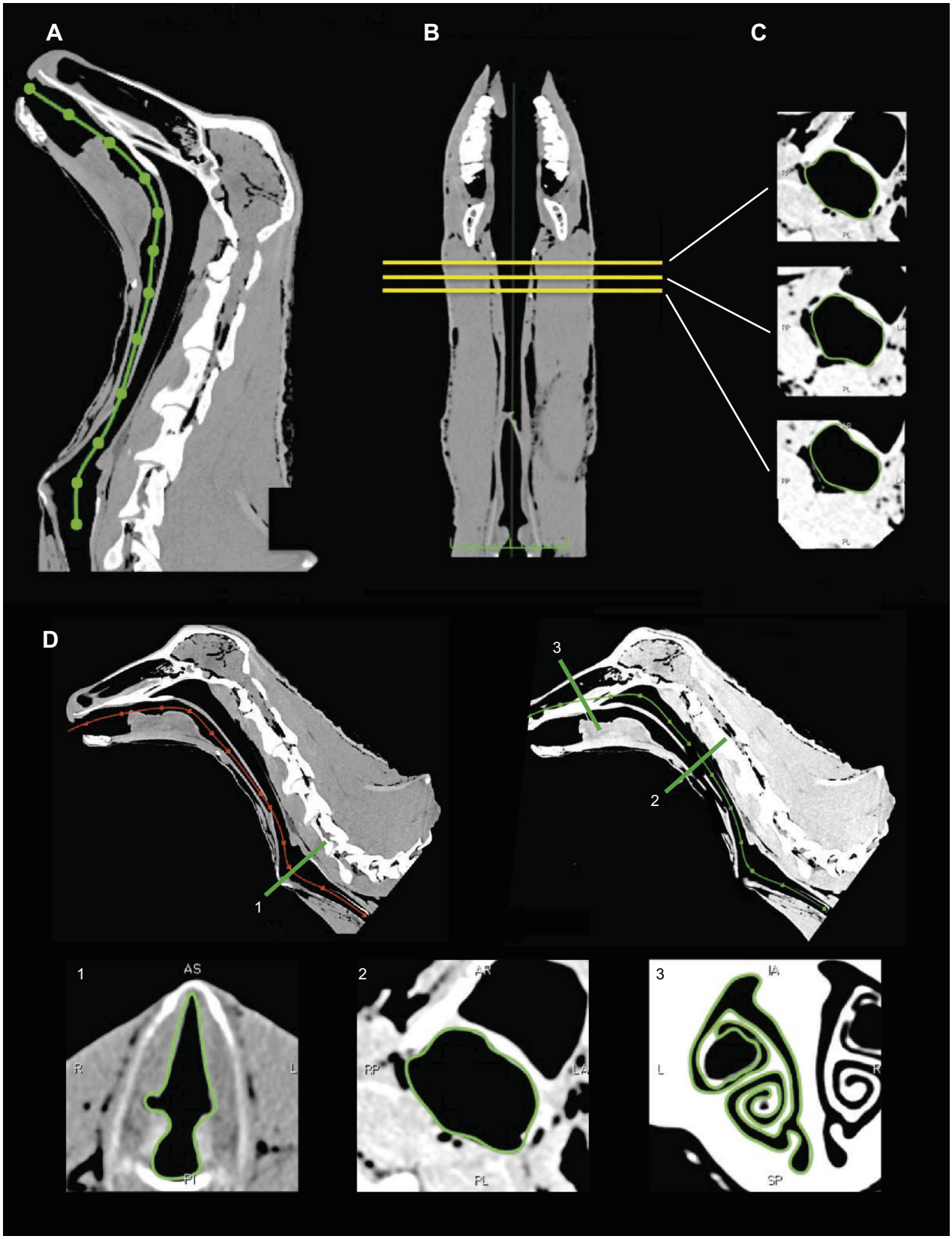

Fig. 3. Multi-planar representation of a CT scan of male 1 illustrating the methodology for measuring the vocal tract area function at maximal artificial extension. (A) Manually drawn dorsoventral and transverse midline through the oral vocal tract. (B) Sampling transverse sections along the virtually stretched, un-curved oral vocal tract in 1 cm steps. (C) Three examples of the obtained cross-sections, highlighting the respective contours of the oral vocal tract in green. (D) Sagittal section of the oral vocal tract (left, midline in red), the nasal vocal tract (right, midline in green) and representative cross-sections at the level of the glottis (1), of the nasopharynx and oropharynx separated by the soft palate (2) and of the nasal cavities (3). R, right; L, left; AS, anterior/superior; PI, posterior/inferior; AR, anterior/right; RP, right/posterior; LA, left/anterior; PL, posterior/left; IA, inferior/anterior; SP, superior/posterior.

Journal of Experimental Biology (2018) 221, jeb179416. doi:10.1242/jeb.179416

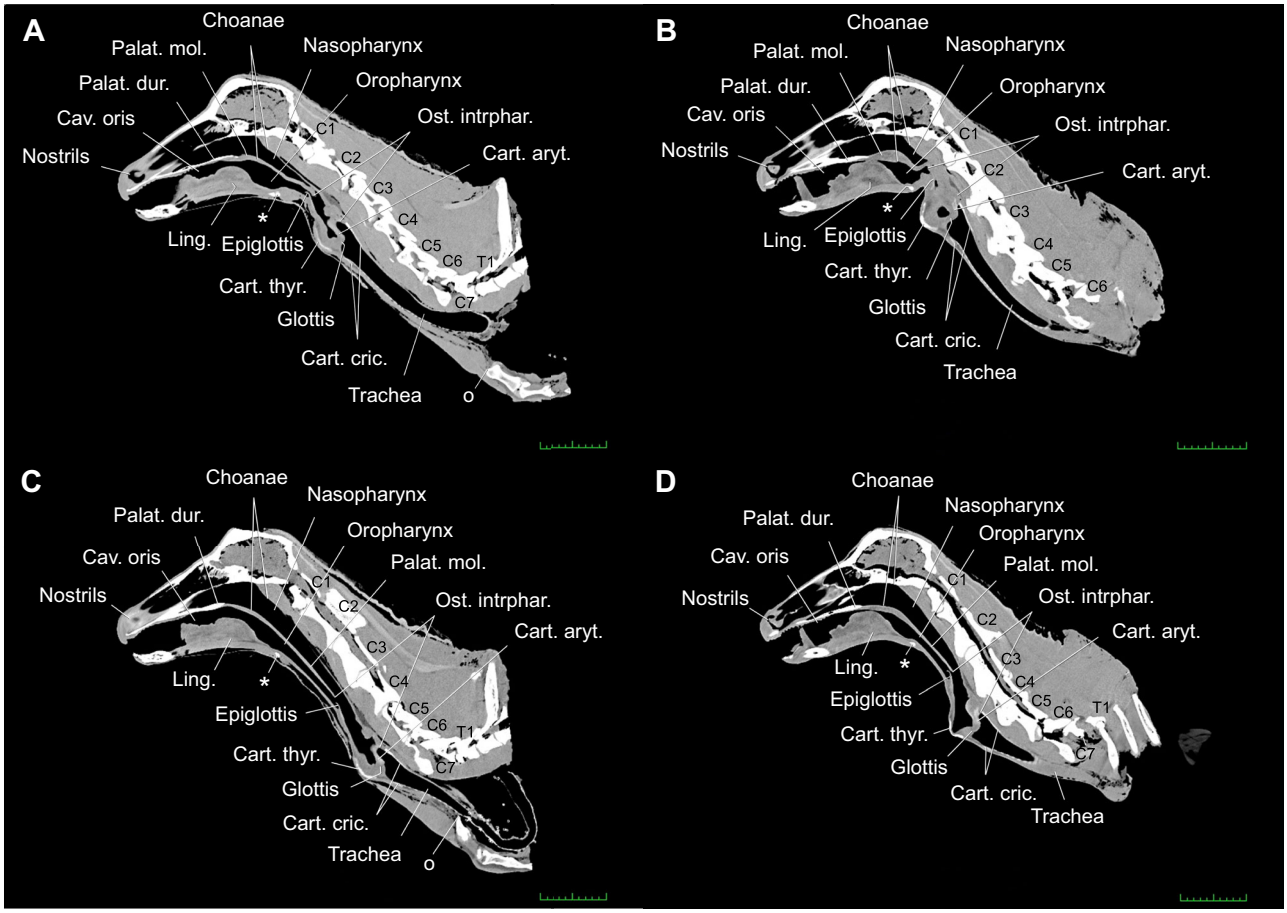

Fig. 4. Midsagittal slices of CT scans of males 1 and 2 with the larynx and vocal tract in a pre-groaning position and in a groaning position. (A,B) Pre-groaning (resting) position; (C,D) groaning position, with the larynx maximally retracted and the vocal tract fully extended. C1–C7 and T1, cervical vertebrae 1–7, first thoracic vertebra; Cart. aryt., arytenoid cartilage; Cart. cric., cricoid cartilage; Cart. thyr., thyroid cartilage; Cav. oris, oral cavity; Choanae, caudal nasal apertures, internal nares; Ling., tongue; Nasopharynx, nasal part of pharynx; Nostrils, rostral nasal apertures, external nares; Oropharynx, oral part of pharynx; Ost. intrphar., intra-pharyngeal ostium (IPO); Palat. dur., hard palate; Palat. mol., soft palate ('velum'); o, rostral tip of sternal manubrium; asterisk, position of the basihyoid. Compared with the resting state, the elongation of the oral and nasal vocal tract is 33% in male 1 (A,C) and 25% in male 2 (B,D). Scale: 10 cm.

is located 41 cm from the lips in male 1 and 34 cm from the lips in male 2. The resting oral vocal tract length (glottis to lips) is 36 cm in male 1 and 30 cm in male 2, and the resting nasal vocal tract length (glottis to nostrils) is 40 cm in male 1 and 35 cm in male 2 (Figs 4 and 5). The flexible region between the rostral edge of the thyroid cartilage and the base of the epiglottis is relaxed and short (4 cm in both male 1 and male 2). Correspondingly, the overall length of the larynx (from cricoid arch to epiglottal tip) is 13 cm in male 1 and 10 cm in male 2. The hyoid apparatus is folded and the distance between the basihyoid and the epiglottis is small (4.5 cm in male 1 and 2.5 cm in male 2). The rostral edge of the intra-pharyngeal ostium (the caudal tip of the palatine velum) is located about 30 cm from the lips in male 1 and 25 cm from the lips in male 2. The epiglottis is in contact with the intra-pharyngeal ostium or overlaps its rostral edge, so that the laryngeal entrance comes to lie in continuation of the nasopharynx (so-called 'intranarial position'). The mouth is mostly closed.

In the extended phonatory configuration (Figs 1B, 2B, 3A,D and 4C,D), the pharynx, soft palate and thyrohyoid ligament are maximally extended, and the larynx resides at the level of cervical vertebrae 4, 5 and 6 in male 1 and 3, 4 and 5 in male 2. Accordingly, the rostral end of the trachea is located approximately 54 cm from the lips in male 1 and 44 cm from the lips in male 2. The extended oral vocal tract length (glottis to lips) is 48 cm in male 1 and 40 cm in male 2, and the extended nasal vocal tract length (glottis to nostrils) is 50 cm in male 1 and 43 cm in male 2 (Figs 4C,D and 5). The length of the common laryngopharyngeal tract (glottis to intra-pharyngeal ostium) is 12 and 9 cm for males 1 and 2, respectively (Figs 4C,D and 5). The flexible region between the rostral edge of the thyroid cartilage and the base of the epiglottis is maximally tensed and considerably elongated (7.5 cm in male 1 and 5 cm in male 2). Correspondingly, the overall length of the larynx (from cricoid arch to epiglottal tip) is 15 cm in male 1 and 13 cm in male 2. The hyoid apparatus is maximally unfolded and the thyrohyoid rotated caudally. The distance between the basihyoid and the epiglottis is considerably enlarged, being now 12 cm in male 1 and 7.5 cm in male 2. The rostral edge of the intra-pharyngeal ostium (the caudal tip of the palatine velum) is located approximately 37 cm from the lips in male 1 and 31 cm in male 2. The epiglottis is retracted from the intra-pharyngeal ostium so that the laryngeal entrance is positioned in continuation of both the oropharynx and nasopharynx. From the intra-pharyngeal ostium onward, the pharyngeal cavity splits into two tubes (the nasopharynx connected to the nasal cavities and the oropharynx connected to the oral cavity) completely separated by the soft palate (velum). The mouth is open for vocalizing.

Journal of Experimental Biology (2018) 221, jeb179416. doi:10.1242/jeb.179416

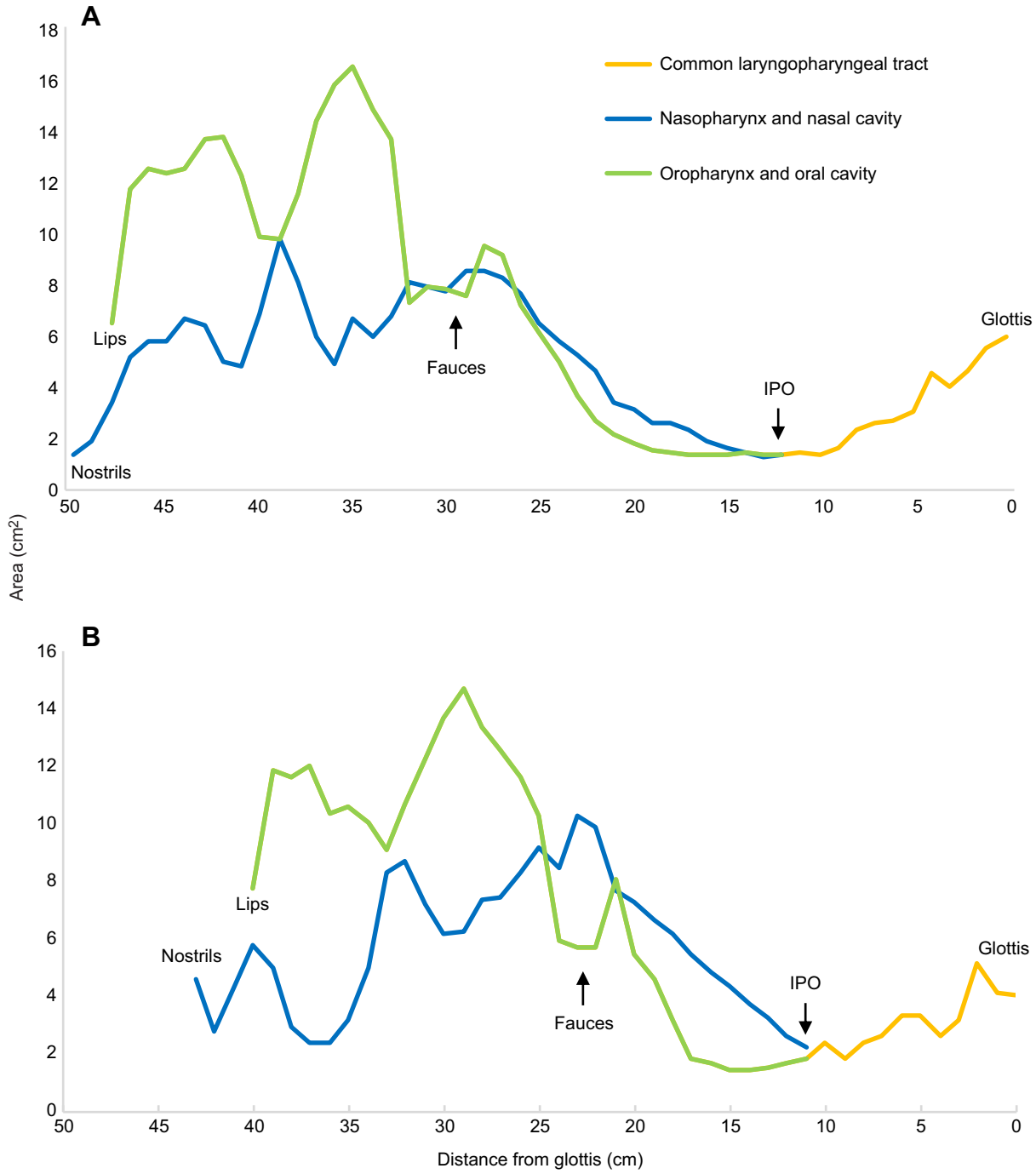

Fig. 5. Estimation of oral and nasal vocal tract cross-sectional area in the maximally extended state, proceeding from right to left. (A) Male 1, (B) male 2. IPO, intra-pharyngeal ostium.

Cross-sectional area

The cross-sectional areas measured along the vocal tracts of each male specimen are shown in Fig. 5. The area functions from the glottis (right) towards the lips and nostrils (left) are highly comparable between the two specimens.

Longitudinally, the choanae and the isthmus faucium are located about 25–30 cm (male 1) and 20–25 cm (male 2) rostral to the glottis, respectively (Fig. 5).

The decrease of the cross-sectional area from the glottis towards the intra-pharyngeal ostium is a consequence of the large larynx of male fallow deer. Its considerable dorsoventral height causes a relatively large intra-laryngeal cross-sectional area at the glottis (Fig. 3D, cross-section 1). From the intra-pharyngeal ostium, the cross-sectional area of the nasopharynx increases towards the choanae and, similarly, the cross-sectional area of the oropharynx increases towards the isthmus faucium. The choanae and isthmus faucium mark the rostral end of the pharynx, i.e. the transition from the nasopharynx to the nasal cavities and from the oropharynx to the oral cavity, respectively. The gradual, mostly uniform increase in cross-sectional area, from the intra-pharyngeal ostium towards the rostral end of the pharynx, reflects the basic funnel shape of the pharynx, which is narrowest at its connection to the larynx

and widest at its connection to the skull and the oral cavity. From the choanae to the nostrils there is an overall decrease of cross-sectional area as a consequence of the narrowing of the nasal cavities towards the muzzle. The particular decrease of cross-sectional area at around 42 cm in male 1 and at around 37 cm in male 2 comes from the ventral nasal conchae, which narrow the nasal cavities by their extensive, scrolled osseous lamellae (Fig. 3D, cross-section 3). From the isthmus faucium to the lips, the cross-sectional area initially increases and then decreases. In between is a particular decrease at around 39 cm in male 1 and around 33 cm in male 2. The initial increase represents the caudal end of the oral cavity between the isthmus faucium and the root of the tongue and the final decrease represents the rostral end of the oral cavity between the lingual fossa and the lips. The intermediate decrease in cross-sectional area results from the lingual torus, an elevation of the tongue in ruminants, which considerably narrows the middle oral cavity. When the mouth is opened and the lower jaw depressed for groan emission, the cross-sectional areas of the (then funnel-shaped) oral cavity will increase accordingly in the direction towards the lips.

Predicted vocal tract resonances

The vocal tract resonances predicted from the vocal tract area functions of male 1 and male 2 and corresponding to the three possible configurations are presented in Fig. 6. Formant F1 predicted by the combined oral and nasal vocal tracts is in an intermediate position between the F1 predicted using the oral vocal tract only and that predicted from the nasal vocal tract only. F2 and F3 predicted by the combined oral and nasal vocal tracts corresponds to the F2 predicted by the nasal vocal tract only, and to the F2 predicted by the oral vocal tract only. F4 and F5 predicted by the combined oral and nasal vocal tracts correspond to the F3 predicted by the nasal vocal tract only, and to the F3 predicted by the oral vocal tract only (Fig. 6, Table 1).

The centre frequencies of each predicted formant are reported in Table 1. The models using both oral and nasal vocal tracts predict much lower formants overall (average formant spacing of 255 Hz) than models using the oral vocal tract only (average formant spacing of 446 Hz) or models using the nasal vocal tract only (average formant spacing of 358 Hz).

Comparison with acoustic observations

Fig. 7 plots the average centre frequencies of the first five formants observed in groans from 16 adult fallow deer males (reported in Vannoni and McElligott, 2007; see Table 2) against the resonances predicted by our three vocal tract models. The resonances predicted by including both the oral and nasal vocal tracts are a better fit to the observed formants than those predicted by using the oral vocal tract or the nasal vocal tract only: the slope of the regression line is closer to 1 (indicating a better fit of the scaling of the resonances) and R^2 is also higher (indicating a better fit of the pattern of the resonances). Examination of the regression slopes in Fig. 7 shows that while model 3 (combined oral and nasal vocal tracts) underestimates DF by 9%, model 1 (oral vocal tract only) overestimates DF by 37% and model 2 (nasal vocal tract only) overestimates DF by 23%. Separate correlations for male 1 and male 2 are given in Fig. S2.

DISCUSSION

In this study, the artificially extended vocal apparatuses of two adult male fallow deer were CT-scanned, and the cross-sectional areas of the complete supra-laryngeal vocal tract (common laryngopharyngeal tract, oropharynx, oral cavity, nasopharynx and nasal cavities) of both specimens were measured along the oral and nasal vocal tracts. We then used this data to model resonance patterns produced by these supra-laryngeal cavities including the oral vocal tract only, the nasal vocal tract only or the combined oral and nasal vocal tracts. We found that the configuration combining the oral and nasal vocal tract geometries produced a resonance pattern which more closely matches the formants observed in fallow deer groans, in terms of both formant frequency pattern and formant frequency scaling.

The formants observed in the groans of fallow deer (Briefer et al., 2010; McElligott and Hayden, 1999) and more generally in the sexually selected calls of male polygynous deer with extensible vocal tracts (Fitch and Reby, 2001; Passilongo et al., 2013; Reby and McComb, 2003; Reby et al., 2016) obey stereotyped, uneven formant patterns incompatible with a vocal tract consisting of a simple linear tube. More specifically, in both fallow deer groans (McElligott et al., 2006) and red deer roars (Reby and McComb, 2003), the second and third formants are close to one another and the fourth formant is higher, leaving a gap between the third and fourth formant. Our simulations combining both the oral and nasal vocal tracts predict this pattern. Comparison of the models suggests that F2 and F4 of fallow deer groans are affiliated to the nasal vocal tract while F3 and F5 are affiliated to the oral vocal tract.

In terms of frequency scaling, our predictions resolve the aforementioned mismatch between apparent vocal tract lengths estimated from formant frequencies measured in fallow deer groans and actual anatomical vocal tract length derived from photogrammetric and anatomical data. Presumably, this is because the inclusion of formants affiliated to the nasal vocal tract led to an overestimation of apparent vocal tract length in previous studies modelling the fallow deer vocal tract as a single uniform tube. Indeed, previous investigations of apparent vocal tract length (i.e. vocal tract length estimated from formant frequencies) in polygynous deer with descended and mobile larynges (Corsican deer: Kidjo et al., 2008; fallow deer: McElligott et al., 2006; Mesola deer: Passilongo et al., 2013; red deer: Reby and McComb, 2003) have modelled the vocal tract as a linear tube with a constant cross-section, closed at one end (glottis) and open at the other (mouth), and excluded the involvement of the nasal vocal tract for loud calls produced with an open mouth. While these succeeded at characterizing inter-individual differences in formant frequency spacing (Kidjo et al., 2008; Vannoni and McElligott, 2007), apparent vocal tract length and thus body size (Reby and McComb, 2003; Vannoni and McElligott, 2008), they probably yielded over-estimations of the anatomical vocal tract length.

The inclusion of nasal resonances in future models should allow for better estimations of apparent vocal tract length from recorded mating calls in these species, thereby potentially enhancing the reliability of bioacoustic tools aimed at assessing body size from vocalizations for research, conservation or wildlife management purposes.

Taken together, our observations strongly suggest that the nasal cavity and oral cavity are simultaneously involved in the vocal production of fallow deer groans. This involvement of the nasal vocal tract due to the non-closure of the intra-pharyngeal ostium during vocal tract extension may be widespread in species with a permanently descended larynx and extensible vocal tract (such as other polygynous deer and goitred gazelles, for example), but also occur in species where callers lower their larynx temporarily for the production of oral (rather than nasal) calls. We suggest that the potential for nasalization of putative oral loud calls should be carefully examined across terrestrial mammals.

Journal of Experimental Biology (2018) 221, jeb179416. doi:10.1242/jeb.179416

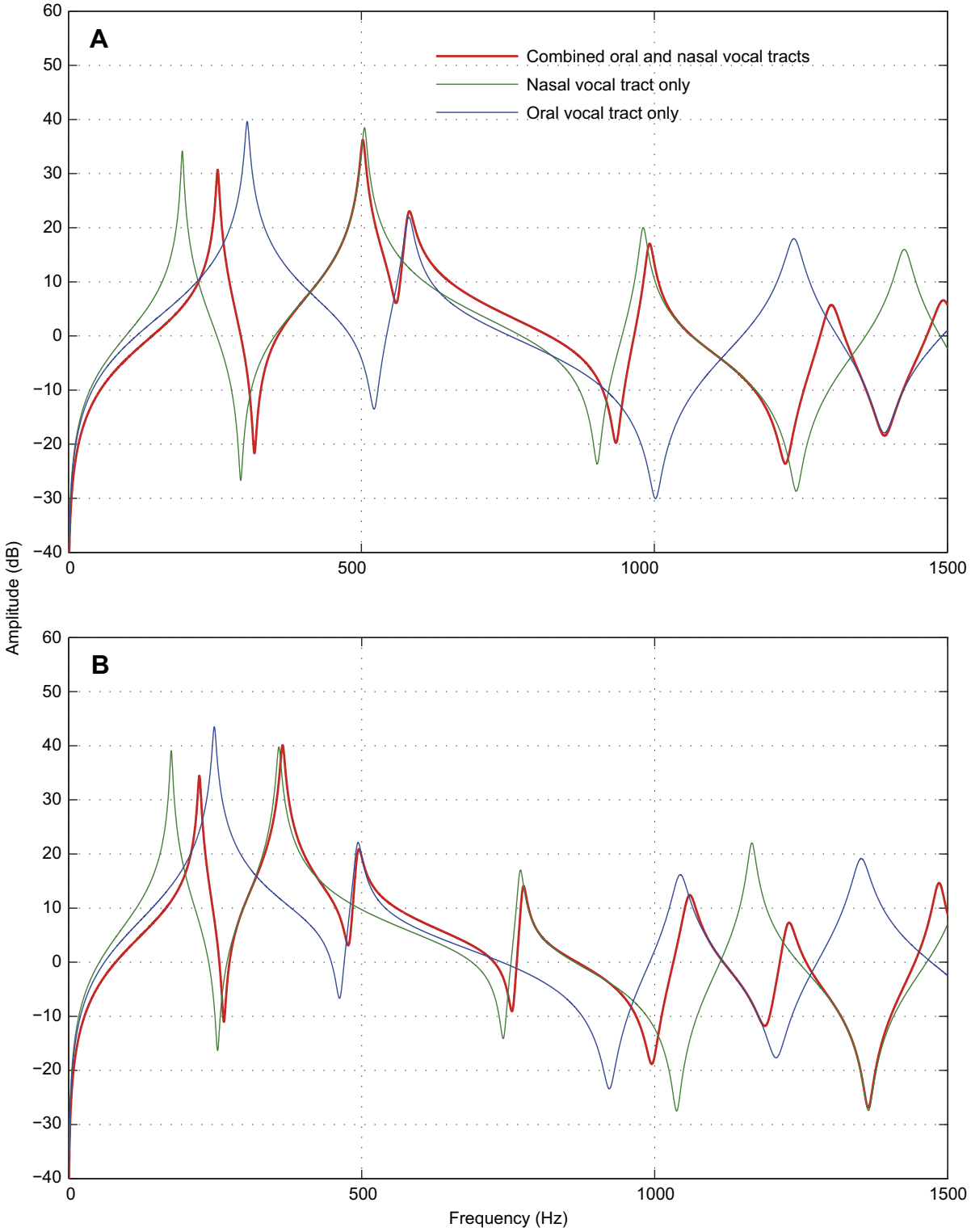

Fig. 6. Predicted resonances for the three possible vocal tract configurations of groan production. (A) Male 1, (B) male 2. Data are for the combined oral and nasal vocal tracts (red), the nasal vocal tract only (green) and the oral vocal tract only (blue). The resonance pattern produced by the combined oral and nasal vocal tracts is more similar to the observed formants in fallow deer groans than the resonance patterns of either the oral or nasal vocal tract alone.

The role of nasal cavities in acoustic output has been investigated in humans using anatomical scans, area functions, vocal tract modelling and/or acoustic analysis (Dang et al., 1994; Feng and Castelli, 1996; Hattori and Fujimura, 1958; Pruthi et al., 2007; Story, 2005). Compared with modulation of the oral vocal tract, nasalization plays a relatively minor role in human speech variation and is often left out of vocal models. However, models that include coupling between the nasal and oral cavity can result in transfer functions that more closely match recorded acoustic output (Dang et al., 1994; Feng and Castelli, 1996). The effects of nasalization are strongest in the lower frequencies (Feng and Castelli, 1996; Pruthi et al., 2007) and include the addition of low-frequency formant peaks as

Journal of Experimental Biology (2018) 221, jeb179416. doi:10.1242/jeb.179416

Table 1. Predicted centre frequencies for formants F1–F5 and estimated formant spacing (DF) for the different vocal tract configurations for males 1 and 2

Configuration	Male	F1 (Hz)	F2 (Hz)	F3 (Hz)	F4 (Hz)	F5 (Hz)	DF (Hz)
Oral vocal tract only	1	249	494	1044	1352	1938	410
	2	305	581	1238	1629	2238	482
Nasal vocal tract only	1	175	359	771	1166	1534	328
	2	194	505	981	1426	1712	388
Combined oral and nasal vocal tracts	1	223	365	495	776	1060	227
	2	255	503	582	992	1302	283

observed here in fallow deer groans. Nasal coupling has also been suggested as a likely mechanism for the addition of low spectral peaks in Diana monkey alarm calls (Riede and Zuberbuhler, 2003).

There are obvious limitations to this investigation. Our dead specimens were scanned in artificial positions constrained by the dimensions of the CT scanner, and thus only approximate the natural postures of live animals during vocalizing. Moreover, the vocal tracts were artificially extended. The geometries are thus approximations of the vocal tract of live animals during vocalizing, and do not account for internal adjustments such as, for example, the possible contribution of palatopharyngeal muscles. Future investigations could involve performing several scans with different combinations of head/neck angle, extent of the laryngeal descent or mouth opening, or perform simulations of these parameters (Gamba et al., 2012; Gamba and Giacoma, 2006b). Using a larger sample of specimens would also allow the assessment of inter-individual variation, including the effect of age or size.

Formant frequencies are known to provide cues to the caller's body size in fallow deer groans and red deer roars, because of the close correlation between formant frequency spacing and body size (McElligott et al., 2006; Reby and McComb, 2003), and are used by male and female receivers to assess rivals and potential mates during the breeding season (Charlton et al., 2007; Charlton et al., 2008a,b; Pitcher et al., 2015; Reby et al., 2005). The descended larynx and extensible vocal tract of fallow and red deer males (and some other species) are therefore considered to be adaptations that allow callers to maximize the acoustic impression of their body size conveyed to receivers (the 'size exaggeration hypothesis': Fitch and Reby, 2001; Ohala, 1984). Our investigations show that the involvement of the nasal vocal tract adds additional formants to the lower part of the spectrum, which increases formant density (decreasing formant spacing), and may make the caller sound larger when compared with oral- or nasal-only calls. Similar functional explanations have been suggested for the evolution of air sacs (de Boer, 2009; Harris et al., 2006), which also increase formant density by adding resonances.

In conclusion, we contend that, while expensive and technically challenging, using 3D CT scanning to predict vocal tract resonances can greatly assist the interpretation of formant patterns in mammalian vocalizations. We suggest that similar

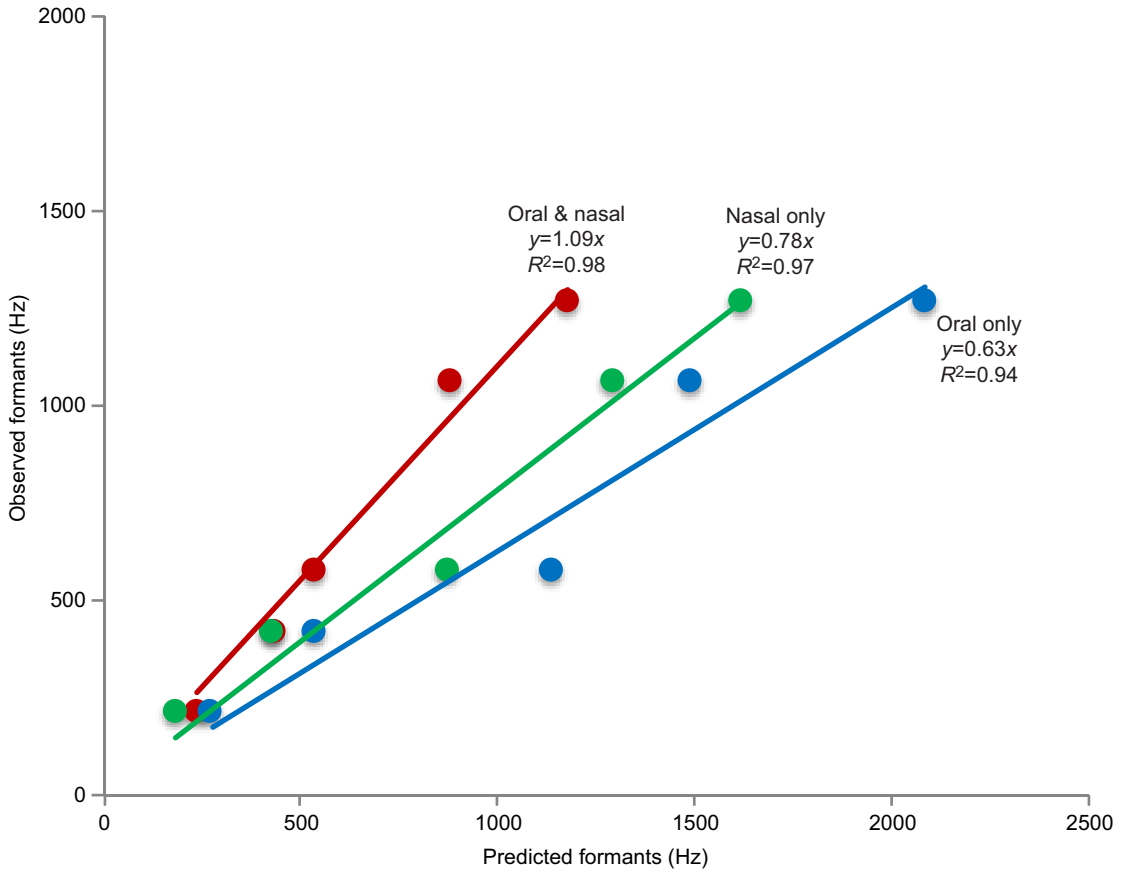

Fig. 7. Correlations between resonances observed in male fallow deer groans (*y*-axis) and resonances predicted from vocal tract geometries of scanned specimens (*x*-axis). Predicted resonances are the average centre frequencies of the first five peaks predicted by the cross-sectional areas of the vocal tract of male 1 and 2, including the oral vocal tract only (blue line), the nasal vocal tract only (green line) or both the oral and nasal vocal tracts (red line). The regression slopes inform the fit of the scaling (formant spacing) of the observed resonances to the predicted resonances. The R^2 values provide the fit of the pattern of the observed resonances to the predicted resonances.

Table 2. Mean centre frequencies for formants F1–F5 and average estimated formant spacing (DF) at maximal vocal tract extension from 16 adult males

	F1 (Hz)	F2 (Hz)	F3 (Hz)	F4 (Hz)	F5 (Hz)	DF
Mean (±s.e.m.) centre frequency (Hz)	208.5±2.0	414.3±1.9	575.2±3.3	1060.2±2.9	1265.9±3.2	300.6±0.8
Minimum centre frequency (Hz)	152	329	457	966	1170	281
Maximum centre frequency (Hz)	263	496	677	1149	1371	326

Data are from Vannoni and McElligott (2007).

approaches could be generalized to the study of vocal tract resonances in other terrestrial mammals.

Acknowledgements
We thank John Bartram, John Comfort and Paul Douglas at the London Royal Parks for their help obtaining the specimens. We are also very grateful to Jan Bush and the amazing staff at the Clinical Imaging Sciences Centre for facilitating the production of the CT scans.

Competing interests
The authors declare no competing or financial interests.

Author contributions
Conceptualization: D.R., J.G.; Methodology: D.R., J.D., J.G.; Software: J.D., J.G.; Formal analysis: D.R., R.F., J.G.; Investigation: D.R., M.W., R.F., J.G.; Resources: D.R., M.W., R.F., J.G.; Data curation: D.R., M.W., R.F., J.G.; Writing - original draft: D.R., M.W., R.F., J.G.; Writing - review & editing: D.R., M.W., R.F., B.C., J.D., J.G.; Supervision: D.R.; Project administration: D.R.; Funding acquisition: D.R.

Funding
J.G. was supported by a Projet International de Coopération Scientifique grant reference 6188 from Centre National de la Recherche Scientifique. D.R. was supported by an invited professorship from Le Mans Université. M.T.W. was supported by a grant from US National Science Foundation International Research Fellowship (grant number 0908569) and an award from the Systematics Research Fund.

Data availability
Supporting data and scripts for predicting vocal tract resonances are available on request from the corresponding author.

Supplementary information
Supplementary information available online at
http://jeb.biologists.org/lookup/doi/10.1242/jeb.179416.supplemental

References
Adam, O., Cazau, D., Gandilhon, N., Fabre, B., Laitman, J. T. and Reidenberg, J. S. (2013). New acoustic model for humpback whale sound production. *Appl. Acoust.* **74**, 1182-1190.
Boë, L.-J., Heim, J., Honda, K. and Maeda, S. (2002). The potential Neandertal vowel space was as large as that of modern humans. *J. Phon.* **30**, 465-484.
Boë, L.-J., Berthommier, F., Legou, T., Captier, G., Kemp, C., Sawallis, T. R., Beckers, Y., Rey, A. and Fagot, J. (2017). Evidence of a vocalic proto-system in the baboon (*Papio papio*) suggests pre-hominin speech precursors. *PLoS ONE* **12**, e0169321.
Briefer, E., Vannoni, E. and McElligott, A. G. (2010). Quality prevails over identity in the sexually selected vocalisations of an ageing mammal. *BMC Biol.* **8**, 1-15.
Carterette, E. C., Shipley, C. and Buchwald, J. (1979). Linear prediction theory of vocalization in cat and kitten. In *Frontiers in Speech Communication Research* (ed. B. Lindblom and S. Ohman), pp. 245-257. New York: Acadcemic Press.
Carterette, E. C., Shipley, C. and Buchwald, J. S. (1984). On synthesizing animal speech: the case of the cat. In *Electronic Speech Synthesis: Techniques, Technology, and Applications* (ed. G. Bristow), pp. 292-302. New York: McGraw-Hill.
Chaigne, A. and Kergomard, J. (2016). *Acoustics of Musical Instruments*. New York: Springer.
Charlton, B., Reby, D. and McComb, K. (2007). Female red deer prefer the roars of larger males. *Biol. Lett.* **3**, 382-385.
Charlton, B., McComb, K. and Reby, D. (2008a). Free-ranging red deer hinds show greater attentiveness to roars with formant frequencies typical of young males. *Ethology* **114**, 1023-1031.
Charlton, B., Reby, D. and McComb, K. (2008b). Effect of combined source (F0) and filter (formant) variation on red deer hind responses to male roars. *J. Acoust. Soc. Am.* **123**, 2936-2943.
Charlton, B., Ellis, W., McKinnon, A., Cowin, G., Brumm, J., Nilsson, K. and Fitch, W. (2011). Cues to body size in the formant spacing of male koala (*Phascolarctos cinereus*) bellows: honesty in an exaggerated trait. *J. Exp. Biol.* **214**, 3414-3422.
Constantinescu, G. M. and Schaller, O. (2012). *Illustrated Veterinary Anatomical Nomenclature*, 3rd edn, pp. 620. Stuttgart: Enke Verlag.
Dang, J. W., Honda, K. and Suzuki, H. (1994). Morphological and acoustical analysis of the nasal and the paranasal cavities. *J. Acoust. Soc. Am.* **96**, 2088-2100.
de Boer, B. (2009). Acoustic analysis of primate air sacs and their effect on vocalization. *J. Acoust. Soc. Am.* **126**, 3329-3343.
de Boer, B. and Fitch, W. T. (2010). Computer models of vocal tract evolution: an overview and critique. *Adapt. Behav.* **18**, 36-47.
Fant, G. (1960). *Acoustic Theory of Speech Production*. The Hague: Mouton.
Feng, G. and Castelli, E. (1996). Some acoustic features of nasal and nasalized vowels: a target for vowel nasalization. *J. Acoust. Soc. Am.* **99**, 3694-3706.
Fitch, W. T. (1997). Vocal tract length and formant frequency dispersion correlate with body size in rhesus macaques. *J. Acoust. Soc. Am.* **102**, 1213-1222.
Fitch, W. T. (2000a). The evolution of speech: a comparative review. *Trends Cogn. Sci.* **4**, 258-267.
Fitch, W. T. (2000b). The phonetic potential of nonhuman vocal tracts: Comparative cineradiographic observations of vocalizing animals. *Phonetica* **57**, 205-218.
Fitch, W. T. and Hauser, M. D. (2002). Unpacking "Honesty": Generating and extracting information from acoustic signals. In *Animal Communication* (ed. A. Megala-Simmons and A. Popper), pp. 65-137. Berlin: Springer-Verlag.
Fitch, W. T. and Reby, D. (2001). The descended larynx is not uniquely human. *Proc. R. Soc. Lond. B Biol. Sci.* **268**, 1669-1675.
Fitch, W. T., de Boer, B., Mathur, N. and Ghazanfar, A. A. (2016). Monkey vocal tracts are speech-ready. *Sci. Adv.* **2**, e1600723-e1600723.
Frey, R. and Gebler, A. (2003). The highly specialized vocal tract of the male Mongolian gazelle (*Procapra gutturosa* Pallas, 1777 - *Mammalia*, *Bovidae*). *J. Anat.* **203**, 451-471.
Frey, R., Gebler, A., Fritsch, G., Nygren, K. and Weissengruber, G. (2007a). Nordic rattle: the hoarse vocalization and the inflatable laryngeal air sac of reindeer (*Rangifer tarandus*). *J. Anat.* **210**, 131-159.
Frey, R., Volodin, I. and Volodina, E. (2007b). A nose that roars: anatomical specializations and behavioural features of rutting male saiga. *J. Anat.* **211**, 717-736.
Frey, R., Volodin, I., Volodina, E., Carranza, J. and Torres-Porras, J. (2012). Vocal anatomy, tongue protrusion behaviour and the acoustics of rutting roars in free-ranging Iberian red deer stags (Cervus elaphus hispanicus). *J. Anat.* **220**, 271-292.
Gamba, M. and Giacoma, C. (2006a). Vocal tract configurations and formant pattern variation in ruffed lemurs vocal production. In Proceedings of the ICVPB 2006, The 5th International Conference on Voice Physiology and Biomechanics, Variations across Cultures and Species, pp. 38-41. Tokyo, Japan.
Gamba, M. and Giacoma, C. (2006b). Vocal tract modeling in a prosimian primate: the black and white ruffed lemur. *Acta Acust. United With Acust.* **92**, 749-755.
Gamba, M., Friard, O. and Giacoma, C. (2012). Vocal tract morphology determines species-specific features in vocal signals of lemurs (*Eulemur*). *Int. J. Primatol.* **33**, 1453-1466.
Harris, T. R., Fitch, W. T., Goldstein, L. M. and Fashing, P. J. (2006). Black and white colobus monkey (*Colobus guereza*) roars as a source of both honest and exaggerated information about body mass. *Ethology* **112**, 911-920.
Hattori, S. and Fujimura, O. (1958). Nasalization of vowels in relation to nasals. *J. Acoust. Soc. Am.* **30**, 267-274.
Kidjo, N., Cargnelutti, B., Charlton, B. D., Wilson, C. and Reby, D. (2008). Vocal behaviour in the endangered Corsican deer: description and phylogenetic implications. *Bioacoustics* **18**, 159-181.
Kim, Y.-C., Narayanan, S. and Nayak, K. (2009). Accelerated 3D MRI of vocal tract shaping using compressed sensing and parallel imaging. In Proceedings of the IEEE International Conference on Acoustical Speech Signal Processing ICASSP 2009, pp. 389-392.
Koda, H., Nishimura, T., Tokuda, I. T., Oyakawa, C., Nihonmatsu, T. and Masataka, N. (2012). Soprano singing in gibbons. *Am. J. Phys. Anthropol.* **149**, 347-355.
Lieberman, P., Crelin, E. S. and Klatt, D. H. (1972). Phonetic ability and related anatomy of the newborn and adult human, Neanderthal man, and the chimpanzee. *Am. Anthropol.* **74**, 287-307.

McElligott, A. G. and Hayden, T. J. (1999). Context-related vocalization rates of fallow bucks, Dama dama. *Anim. Behav.* **58**, 1095-1104.
McElligott, A. G., Birrer, M. and Vannoni, E. (2006). Retraction of the mobile descended larynx during groaning enables fallow bucks (*Dama dama*) to lower their formant frequencies. *J. Zool.* **270**, 340-345.
Ohala, J. J. (1984). An ethological perspective on common cross-language utilization of F0 of voice. *Phonetica* **41**, 1-16.
Passilongo, D., Reby, D., Carranza, J. and Apollonio, M. (2013). Roaring high and low: composition and possible functions of the Iberian stag's vocal repertoire. *PLoS ONE* **8**, e63841.
Pitcher, B. J., Briefer, E. F. and McElligott, A. G. (2015). Intrasexual selection drives sensitivity to pitch, formants and duration in the competitive calls of fallow bucks. *BMC Evol. Biol.* **15**, 149.
Pruthi, T., Espy-Wilson, C. Y. and Story, B. H. (2007). Simulation and analysis of nasalized vowels based on magnetic resonance imaging data. *J. Acoust. Soc. Am.* **121**, 3858-3873.
Reby, D. and McComb, K. (2003). Anatomical constraints generate honesty: acoustic cues to age and weight in the roars of red deer stags. *Anim. Behav.* **65**, 519-530.
Reby, D., Joachim, J., Lauga, J., Lek, S. and Aulagnier, S. (1998). Individuality in the groans of fallow deer (*Dama dama*) bucks. *J. Zool.* **245**, 79-84.
Reby, D., McComb, K., Cargnelutti, B., Darwin, C., Fitch, W. T. and Clutton-Brock, T. H. (2005). Red deer stags use formants as assessment cues during intrasexual agonistic interactions. *Proc. R. Soc. Lond. B Biol. Sci.* **272**, 941-947.
Reby, D., Wyman, M. T., Frey, R., Passilongo, D., Gilbert, J., Locatelli, Y. and Charlton, B. D. (2016). Evidence of biphonation and source-filter interactions in the bugles of male North American wapiti (*Cervus canadensis*). *J. Exp. Biol.* **219**, 1224-1236.
Riede, T. and Zuberbuhler, K. (2003). The relationship between acoustic structure and semantic information in Diana monkey alarm vocalization. *J. Acoust. Soc. Am.* **114**, 1132-1142.
Riede, T., Bronson, E., Hatzikirou, H. and Zuberbuhler, K. (2005). Vocal production mechanisms in a non-human primate: morphological data and a model. *J. Hum. Evol.* **48**, 85-96.
Story, B. H. (2005). A parametric model of the vocal tract area function for vowel and consonant simulation. *J. Acoust. Soc. Am.* **117**, 3231-3254.
Taylor, A., Charlton, B. D. and Reby, D. (2016). Vocal production by terrestrial mammals: source, filter and function. In *Vertebrate Sound Production and Acoustic Communication* (ed. R. A. Suthers, W. T. Fitch, R. R. Fay and A. Popper). Berlin: Springer International Publishing.
Titze, I. R. (1989). Physiologic and acoustic differences between male and female voices. *J. Acoust. Soc. Am.* **85**, 1699-1707.
Titze, I. R. (1994). *Principles of Voice Production*. Englewood Cliffs, New Jersey: Prentice Hall.
Vannoni, E. and McElligott, A. G. (2007). Individual acoustic variation in fallow deer (*Dama dama*) common and harsh groans: a source-filter theory perspective. *Ethology* **113**, 223-234.
Vannoni, E. and McElligott, A. G. (2008). Low frequency groans indicate larger and more dominant fallow deer (*Dama dama*) males. *PLoS ONE* **3**, e3113.

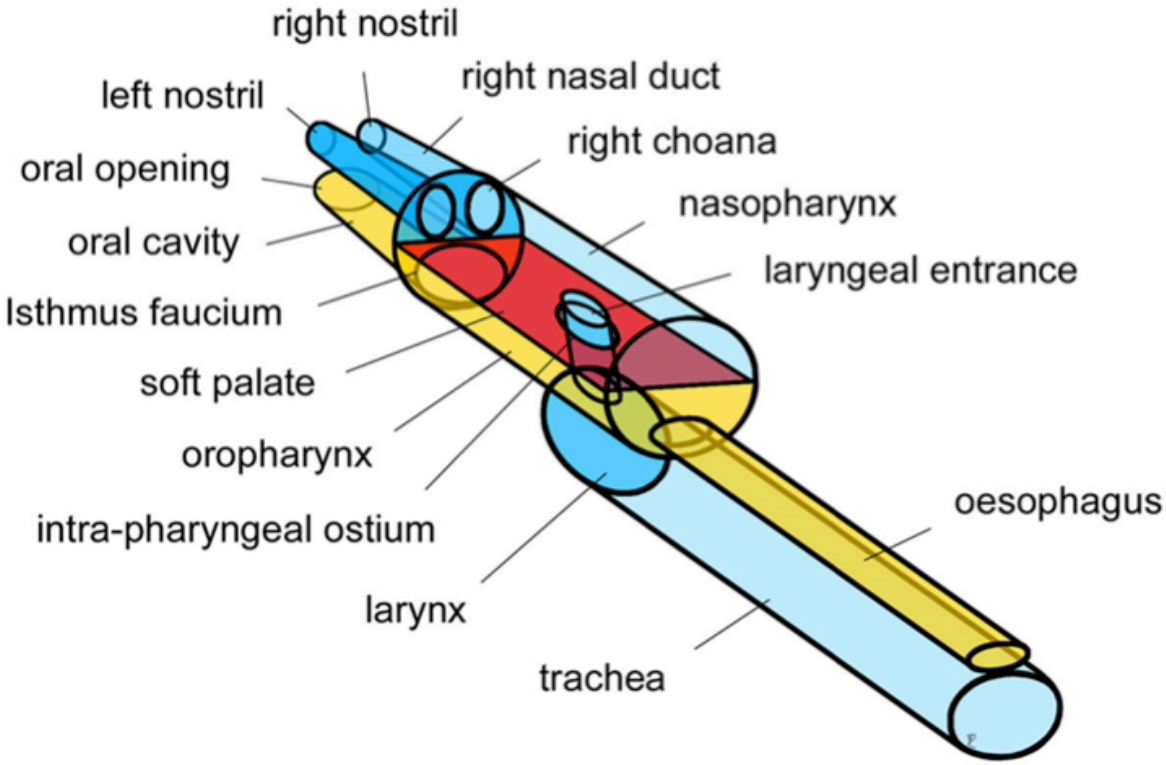

Fig. S1. Model of a mammalian vocal tract.
The model demonstrates that the most rostral portions of the nasal vocal tract are paired (left and right nostril, left and right nasal duct) up to the choanae. Then, from the choanae along the nasopharynx, the nasal vocal tract becomes unpaired, enters the larynx and ends at the vocal folds inside the larynx. Caudally subsequent to the larynx, the trachea connects the upper airways to the lungs.

Typically, the intra-pharyngeal ostium in mammals is a simple oval opening in the soft palate that connects the nasal vocal tract to the oral vocal tract. It is the single opening by which the naso- and oropharynx communicate. Through this opening, the entrance of the larynx protrudes into the nasopharynx during quiet breathing.

The oral vocal tract is unpaired throughout. The most rostral portion comprises the lips and the oral opening followed by the oral cavity and the isthmus of the fauces at the transition to the oropharynx. After having passed the oropharynx, the oral vocal tract also enters the larynx. This can only occur when the larynx is withdrawn from the intra-pharyngeal ostium and the laryngeal entrance then lies inside the oropharynx, e.g. for producing an open-mouth call. As the intra-laryngeal portion of the nasal vocal tract the oral vocal tract ends at the vocal folds inside the larynx.

The soft palate produces a complete subdivision of the pharynx in a two-storey tube (cf.: Wood Jones 1940: The nature of the soft palate. J Anat Physiol 74, 147-170.). The dorsal nasopharynx continues through the intra-pharyngeal ostium and the larynx into the ventrally located trachea. The ventral oropharynx continues around the epiglottis and the laryngeal entrance into the dorsally located oesophagus (crossing of airway and foodway). Caudally subsequent to the oropharynx, the oesophagus courses dorsal to the larynx and trachea.

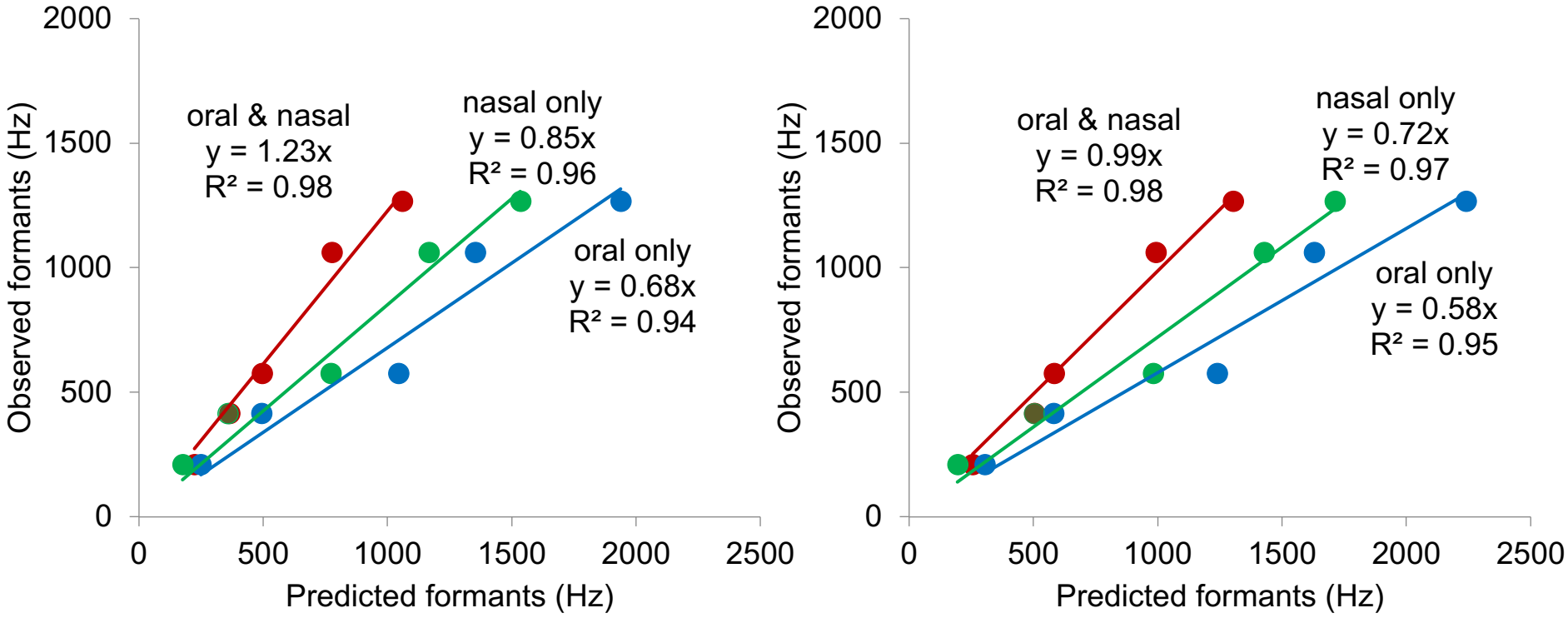

Fig. S2. Correlations between resonances observed in male fallow deer groans (y axis) as reported in the literature and resonances predicted from vocal tract geometries (x axis) for two scanned specimens, male 1 (left) and male 2 (right). Predicted resonances are the average centre frequencies of the first 5 peaks predicted by the cross-sectional areas of the vocal tract of male 1 and 2 including the oral vocal tract only (blue line), the nasal vocal tract only (green line), or both the oral and nasal vocal tracts (red line). Observed resonances are the average centre frequencies calculated from 16 males (Vannoni & McElligott 2007). The regression slopes inform the fit of the scaling (formant spacing) of the observed resonances to the predicted resonances. The values of R^2 provide the fit of the pattern of the observed resonances to the predicted resonances.

While the formant frequencies predicted by combined oral and vocal tract geometries are an excellent match to formant frequencies reported in the literature in male 2, those predicted for male 1 underestimate those observed by 23%, suggesting that the vocal tract may have been excessively artificially extended before CT-scanning.